Gene Expression in Kidney Cancer Is Associated with Cytogenetic Abnormalities, Metastasis Formation, and Patient Survival

Holger Sültmann, Anja von Heydebreck, Wolfgang Huber, et al.

Clin Cancer Res 2005;11:646-655.

Gene Expression in Kidney Cancer Is Associated with Cytogenetic Abnormalities, Metastasis Formation, and Patient Survival

Holger Sültmann,[1] Anja von Heydebreck,[2] Wolfgang Huber,[1] Ruprecht Kuner,[1] Andreas Buneß,[1] Markus Vogt,[1] Bastian Gunawan,[3] Martin Vingron,[2] Laszlo Füzesí,[3] and Annemarie Poustka[1]

[1]Division of Molecular Genome Analysis, German Cancer Research Center, Heidelberg, Germany; [2]Department of Computational Molecular Biology, Max-Planck-Institute for Molecular Genetics, Berlin, Germany; and [3]Institute of Pathology, University of Göttingen, Göttingen, Germany

ABSTRACT

Current diagnosis of renal cancer consists of histopathologic examination of tissue sections and classification into tumor stages and grades of malignancy. Until recently, molecular differences between tumor types were largely unknown. To examine such differences, we did gene expression measurements of 112 renal cell carcinoma and normal kidney samples on renal cell carcinoma–specific cDNA microarrays containing 4,207 genes and expressed sequence tags. The gene expression patterns showed deregulation of complete biological pathways in the tumors. Many of the molecular changes corresponded well to the histopathologic tumor types, and a set of 80 genes was sufficient to classify tumors with a very low error rate. Distinct gene expression signatures were associated with chromosomal abnormalities of tumor cells, metastasis formation, and patient survival. The data highlight the benefit of microarrays to detect novel tumor classes and to identify genes that are associated with patient variables and tumor properties.

INTRODUCTION

Adult kidney cancer [renal cell carcinoma (RCC)] is one of the 10 most common human malignancies in developed countries. Its global incidence has been increasing continuously during the past 30 years (1). Males are afflicted twice as often compared with females, and several genetic factors, such as the *VHL* gene, are known to play a role in a subset of RCC. Histologically, RCC is divided into clear cell (ccRCC), papillary (pRCC), chromophobe cell (chRCC), and Bellini duct carcinoma (2, 3). The two most frequent types, ccRCC (80%) and pRCC (10%), originate from the proximal tubules, whereas chRCC (5%) are thought to be derived from the cortical collecting ducts. The histomorphologic tumor types correlate with specific chromosomal abnormalities (1, 4, 5). Most ccRCC are characterized by loss of chromosome 3p (6, 7), whereas gains of chromosomes 7 and 17 are typical for pRCC (8, 9). Losses of chromosomes 1, 2, 6, 10, 13, and 17 are seen in chRCC (10). The chromosomal changes are accompanied by deletions or amplifications of prominent genes in the corresponding regions [i.e., the *VHL* tumor suppressor gene (3p) in ccRCC and the *HPRCC* (7q) in pRCC]. Apart from these typical markers, other genes known to be involved in renal cancer include *VEGF* (11, 12), *EGFR* (13, 14), *TGFA* (15), *MYC* (16, 17), and *VIM* (18).

Novel developments in the Human Genome Project enable more detailed analyses of molecular profiles of tumors and tumor prognosis. In particular, array-based technologies permit large-scale gene expression analysis. Consequently, the list of genes potentially involved in RCC formation and progression has expanded considerably in the recent past (19–23). In a previous study (19), we used array-based gene expression analyses to identify differential gene expression between RCC and the corresponding normal tissues. Here, we used these data to construct RCC-specific microarrays encompassing 4,207 cDNA clones and hybridized these with 87 RCC and 25 normal kidney samples. The aims of the present study were to find gene expression patterns distinguishing among the three major types of RCC and to identify novel tumor subgroups. In addition, molecular changes were compared with tumor variables and patient outcome to identify new marker genes for RCC diagnosis and prognosis.

MATERIALS AND METHODS

Tissue Samples and RNA Isolation. A total of 87 tumors (65 ccRCC, 13 pRCC, and 9 chRCC) and 25 normal kidney tissues (Table 1) were collected between 1996 and 2002.[4] Viable tissue samples were excised by pathologists immediately after surgery. Parts of the tumors were snap frozen in liquid nitrogen and stored at −80°C. Total cellular RNA was isolated by Trizol (TriFast, peqlab, Erlangen, Germany) following homogenization with a Micro-Dismembrator S (Braun Biotech, Melsungen, Germany). RNA quality was checked with the Agilent 2100 bioanalyzer (Agilent Technologies GmbH, Waldbronn, Germany). More than 90% of all samples yielded high-quality RNA (28S/18S rRNA and E_{260}/E_{280} ratios close to 2) and were selected for the experiments. Low-quality RNA samples were

Received 5/14/04; revised 9/29/04; accepted 10/13/04.
Grant support: German Federal Ministry for Education and Research in the German Human Genome Project grant 01KW9911/9.
The costs of publication of this article were defrayed in part by the payment of page charges. This article must therefore be hereby marked *advertisement* in accordance with 18 U.S.C. Section 1734 solely to indicate this fact.
Note: Supplementary data for this are available at Clinical Cancer Research Online (http://clincancerres.aacrjournals.org/). Data accessibility: The microarray data reported in this article were submitted to the ArrayExpress database (http://www.ebi.ac.uk/arrayexpress/) and assigned the accession no. E-DKFZ-1.
Requests for reprints: Holger Sültmann, Division of Molecular Genome Analysis, German Cancer Research Center, Im Neuenheimer Feld 580, D-69120 Heidelberg, Germany. Phone: 49-6221-424705; Fax: 49-6221-42524705; E-mail: h.sueltmann@dkfz.de.

[4] The experiments were done in accordance with the German ethical requirements and were approved by the Ethics Commission of the University of Göttingen (March 6, 2002).

not used and are not listed in Table 1. Other tumor parts were subjected to routine histopathologic examination and cytogenetic analysis as described previously (7).

Microarray Experiments. The microarrays used consisted of 1,794 clones for oncologically relevant genes and 2,314 differentially expressed genes and expressed sequence tags (EST) reported in ref. 19. With additional control genes, the microarrays contained 4,207 genes and ESTs. PCR products from cDNA clones were purified by isopropanol precipitation, washed in 70% ethanol, and dissolved in 3× SSC/1.5 mol/L betaine. The DNA was spotted in duplicate on silanized or poly-L-lysine coated glass slides (Quantifoil, Jena, Germany, and Sigma Diagnostics, Deisenhofen, Germany, respectively) using the Omnigrid (Genemachines, San Carlos, CA) spotter and SMP3 pins (Telechem, Sunnyvale, CA). After spotting, microarrays were rehydrated, and DNA was denatured with boiling water before washing with 0.2% SDS, water-ethanol, and isopropanol. The arrays were dried with pressure air.

RNA Labeling and Hybridization. Ten micrograms of total RNA were mixed with 1 μg $(dT)_{17}$ primer, incubated at 70°C for 10 minutes, and cooled on ice. The labeling reaction was done in a 12.5 μL mixture containing 2.5 μL of 5× RT buffer (Invitrogen, Karlsruhe, Germany), 1.25 μL of 0.1 mol/L DTT, 1 μL each of 5 mmol/L deoxynucleotide triphosphate mix (dGAT), 0.5 μL of 3 mmol/L dCTP, 0.5 μL (20 units) RNasin, 0.5 μL of 1 mmol/L Cy3- or Cy5-labeled dCTP (Amersham Pharmacia Biotech, Freiburg, Germany), and 1 μL (100 units) SuperScript II reverse transcriptase (Invitrogen). The mixture was incubated for 1 hour at 42°C, and the reaction was stopped by addition of 1.25 μL of 50 mmol/L EDTA (pH 8). The RNA was removed by hydrolysis with 5 μL of 1 mol/L NaOH at 65°C for 10 minutes followed by neutralization with 1 μL of 5 mol/L acetic acid. Cy3- and Cy5-labeled samples were combined, precipitated with 100 μL isopropanol at −20°C for 30 minutes, and centrifuged at 13,000 rpm for 15 minutes. The pellet was washed with 70% ethanol, air-dried, and dissolved in 30 μL of 1× DIG-Easy hybridization buffer (Roche Diagnostics, Mannheim, Germany) containing 5× Denhardt's solution and 10 ng/μL Cot1-DNA (Invitrogen). The sample was heat denatured (65°C, 2 minutes) and hybridized with the DNA on microarrays in a hybridization chamber (overnight, 37°C). The slides were washed with 1× SSC/0.1% SDS (15 minutes) and 0.1× SSC/0.1% SDS (10 minutes) and cleaned by 70% and 95% ethanol before drying with pressure air.

Image Quantification and Data Analysis. Arrays were scanned with the GenePix 4000B microarray scanner (Axon Instruments, Inc., Union City, CA), and spots were quantified using Arrayvision 6.0 software (Imaging Research, Inc., St. Catharines, Ontario, Canada). Background-corrected intensity values were normalized and transformed to generalized log ratios through the variance stabilization method (24). Values from duplicate spots for each cDNA clone were averaged.

To identify differentially expressed genes in the tumor-normal comparison, the Significance Analysis of Microarrays software package (25) was used. The software system R (26) was used for all other analyses. We first did complete linkage hierarchical clustering with respect to Euclidean distance applied to the rows (representing genes) and columns (representing samples) of the expression data matrix. Second, we ran the classification method prediction analysis for microarrays (ref. 27; pamr version 1.13) to classify tumor subgroups by gene expression patterns. Standard statistical tests were used to investigate the association of gene expression with clinicopathologic variables. In two-class comparisons, the two-sample *t* test was used. To identify genes of which expression was correlated with tumor type, a *F* test was conducted for each gene. Tests for association of gene expression with the number of chromosomal changes were based on gene-wise linear models. In the analysis of patient survival times, a Cox proportional hazard model was fitted for each gene. In all cases, the expected proportion of false positives using a given cutoff point of the test statistic (false discovery rate) was estimated using random permutations of the sample labels (28).

Real-time PCR. Quantitative real-time PCR was done using the ABI Prism 7900HT Sequence Detection System (Applied Biosystems, Weiterstadt, Germany) and gene-specific primers and probes. cDNAs of six randomly chosen samples of the same cohort (Table 1) each from normal kidney tissue, ccRCC, chRCC, and pRCC were prepared and diluted to 1 ng/μL. Triplicate reactions were run in a 20 μL volume according to the instructions of the supplier. Standard curves were prepared through a cDNA dilution series for every gene. For each sample, the mean C_t value and the SD were calculated from the triplicates. Gene expression levels were determined by relative quantification (29) using *COPB* or *ACTB* as an internal control gene for normalization and normal kidney tissue as a calibrator (expression level set to 1).

RESULTS

The microarray study was divided into two experimental series (Table 1). In the first experiment, we hybridized the RCC-specific microarrays with 74 Cy3-labeled RCC samples (52 ccRCC, 13 pRCC, and 9 chRCC). A Cy5-labeled sample pool of 28 tumor RNA samples (15 ccRCC, 5 chRCC, and 8 pRCC) was used as a common reference for these hybridizations. In the second experiment, we hybridized 25 primary ccRCC samples and 25 normal kidney samples from the same patients.

Gene Expression Widely Correlates with Tumor Types. First, to analyze gene expression among ccRCC, pRCC, and chRCC, we did a *F* test for each gene over all samples. Here, 1,224 genes and ESTs were significantly different between the tumor types ($P < 0.005$; estimated false discovery rate = 0.007; Supplementary Table S1), which suggested a clear molecular discrimination between the three tumor types. Second, we did complete linkage hierarchical clustering of genes and samples using the 100 genes with the highest variances across all samples. This unsupervised analysis resulted in a clustering of the samples that corresponded well to the histopathologic tumor types (Fig. 1, Supplementary Table S2). The 100 genes could be divided into five clusters discriminating the tumor types (Fig. 1). Clusters 1 and 2 consisted of genes or ESTs that were mainly down-regulated in pRCC and chRCC compared with ccRCC. Among these were genes for metabolic processes (*GAPD*), angiogenesis (*ANGPTL4* and *VEGF*), cell adhesion (*COL3A1* and *FN1*), and immune response (*IGHG3* and *HLA-DRB1*). Cluster 3 genes (mainly ESTs) were up-regulated in pRCC and chRCC compared with ccRCC, whereas cluster 4 genes were

Table 1 Patients and samples used in this study

ID	Tumor type	Age (y)/sex	Tumor size (cm)	Tumor stage (tumor-node-metastasis)	Grade	Follow-up (mo)	Cytogenetic changes	Analysis used for tumor classification	Analysis used for tumor-normal comparison
1	pRCC	59/M	1.5	I (T_{1a},N_0,M_0)	2	NED, 20	−Y, +7, +16, +17, +20	X	
2	pRCC	81/M	2.5	I (T_{1a},N_0,M_0)	1	NED, 46	+2, +3, +5, +7, +7, +8, +12, +12, +16, +17, +20	X	
3	pRCC	48/M	3	I (T_{1a},N_x,M_x)	2	NA	NA	X	
4	pRCC	75/F	5.5	I (T_{1b},N_x,M_x)	2	NED, 7	+2, +3, +7, +7, +12, +13, +16, +17, +20, +22	X	
5	pRCC	72/M	8	II (T_2,N_0,M_0)	2	NED, 46	−Y, +7, +16, +17, +20	X	
6	pRCC	59/M	4.5	III (T_{3a},N_0,M_0)	2	NED, 54	−Y, +2, −11q, −14, +16, +17, +20	X	
7	pRCC	65/F	8	III (T_{3b},N_0,M_0)	1	NED, 63	+12, +16, +17	X	
8	pRCC	61/M	12	III (T_{3b},N_x,M_0)	2	NED, 23	−Y, −8p, −15, −15q, +16p, +16p, −16q, −17p, +17q, +17q, −19p, −22	X	
9	pRCC	54/M	4	III (T_{1a},N_1,M_0)	1	AD, 48	+X, +3, +7, +8, +16, +17	X	
10	pRCC	46/M	13	III (T_{3a},N_1,M_x)	3	AD, 3	+3, +7, +10, +16, +17, +20	X	
11	pRCC	74/M	5	IV (T_{3b},N_1,M_1)	3	DOTD, 0	+1q, +1q, −2, +3p, +7, +12p, +12q, +12q, +16, +17, +19, +20, +20	X	
12	pRCC	70/M	2.5	IV (T_{1a},N_2,M_1)	2	AD, 9	−Y, +3, +7, +7, −8p, +12, −18, +20	X	
13	pRCC	71/F	2	IV (T_{1a},N_2,M_1)	2	DOTD, 4	+3, +7, +16, +17, +20	X	
14	chRCC	76/F	2.5	I (T_{1a},N_x,M_x)	1	NA	−X, −1, −2, −6, −10, −13, −17	X	
15	chRCC	60/M	3	I (T_{1a},N_x,M_x)	2	NED, 1	NA	X	
16	chRCC	46/M	5	I (T_{1b},N_x,M_x)	2	NA	NA	X	
17	chRCC	51/M	6	I (T_{1b},N_x,M_x)	2	NA	NA	X	
18	chRCC	26/F	6.5	I (T_{1b},N_x,M_x)	1	NA	NA	X	
19	chRCC	37/M	8	II (T_2,N_x,M_x)	2	NA	−Y, −1, −2, −6, −10, −13, −17, −18, −21	X	
20	chRCC	47/M	9	II (T_2,N_x,M_x)	2	NA	NA	X	
21	chRCC	60/F	12	II (T_2,N_0,M_x)	2	NED, 26	NA	X	
22	chRCC	63/F	12	III (T_{3a},N_1,M_x)	3	AD, 7	−X, −1, −2, −6, −10, −11, −13, −14p, −17	X	
23	ccRCC	66/M	1.5	I (T_{1a},N_0,M_0)	2	NED, 33	−3, −4p, +5q, +7, −14	X	
24	ccRCC	58/F	3	I (T_{1a},N_x,M_x)	2	NED, 42	−X, der(3)t(3;5)	X	
25	ccRCC	38/M	3.5	I (T_{1a},N_0,M_0)	2	NED, 24	−3, −14, +18, +21	X	
26	ccRCC	81/F	4	I (T_{1a},N_0,M_0)	2	DOTD, 26	−3p, −8p, +8q, −9, −14, +16	X	
27	ccRCC	58/M	4	I (T_{1a},N_x,M_x)	2	NA	−Y, −3, −4, −6, −10, −14, −16, −17, −18	X	
28	ccRCC	42/M	4	I (T_{1a},N_x,M_x)	1	NED, 5	−3p, −10q, −9q, −10	X	
29	ccRCC	52/M	5	I (T_{1b},N_0,M_0)	2	NED, 9	−Y, +2 q, −3p	X	X
30	ccRCC	62/M	5	I (T_{1b},N_x,M_x)	1	NED, 1	der(3)t(3;5), −14	X	
31	ccRCC	72/M	5	I (T_{1b},N_0,M_0)	1	NED, 12	−3, +3q, −6q	X	
32	ccRCC	62/M	5.5	I (T_{1b},N_0,M_x)	2	NA	−1p, der(3)t(3;5), +5, +7, +7, +12, +15, +20	X	
33	ccRCC	54/F	6	I (T_{1b},N_0,M_0)	2	NED, 2	+X, der(3)t(3;5), −4	X	
34	ccRCC	58/M	8	II (T_2,N_0,M_0)	2	NED, 11	−Xp, −3p, −6, −8p, −15q	X	
35	ccRCC	62/M	8.8	II (T_2,N_0,M_0)	2	NED, 5	−1p, der(3)t(3;5), +der(3)t(3;5), +12, −14	X	X
36	ccRCC	60/M	10	II (T_2,N_x,M_x)	2	NED, 3	−Y, +2q, −3, +3q, +7q, −9, −14	X	X
37	ccRCC	43/M	12	II (T_2,N_x,M_x)	2	NED, 4	−2q, der(3)t(3;5), +8q	X	
38	ccRCC	51/M	3.5	III (T_{1a},N_1,M_0)	2	DOTD, 321	+2q, der(3)t(3;5), −14	X	
39	ccRCC	59/M	10	III (T_{3a},N_0,M_0)	2	NED, 36	der(3)t(3;5), −10q	X	X
40	ccRCC	85/M	9.5	III (T_{3a},N_x,M_x)	2	DP, 15	+2, −3, +3q, −6q, +7	X	
41	ccRCC	61/F	2.7	III (T_{3b},N_x,M_x)	1	NED, 48	−3p, +5	X	
42	ccRCC	63/M	4.5	III (T_{3b},N_x,M_0)	1	DP, 56	−Y, der(3)t(3;5), −14	X	
43	ccRCC	62/M	5	III (T_{3b},N_0,M_0)	2	NED, 26	−Y, der(3)t(3;5), −15p	X	
44	ccRCC	75/M	6	III (T_{3b},N_x,M_x)	3	DP, 12	−Xq, −Y, +2q, −6, −8, −16, −17, −18, −19, −21, −22	X	
45	ccRCC	56/F	6	III (T_{3b},N_0,M_x)	2	NA	−3, +3q, −16q	X	

(*Continued on the next page*)

Table 1 Patients and samples used in this study (Cont'd)

ID	Tumor type	Age (y)/sex	Tumor size (cm)	Tumor stage (tumor-node-metastasis)	Grade	Follow-up (mo)	Cytogenetic changes	Analysis used for tumor classification	Analysis used for tumor-normal comparison
46	ccRCC	57/F	6	III (T_{3b},N_x,M_x)	2	NA	−3p	X	
47	ccRCC	56/M	6	III (T_{3b},N_0,M_0)	2	NED, 29	−3, −14p, −14q, −18q	X	
48	ccRCC	70/F	8	III (T_{3b},N_0,M_0)	2	NED, 19	−1p, der(3)t(3;5), −4, −8, −9, −14, −21p	X	X
49	ccRCC	67/M	8	III (T_{3b},N_x,M_x)	2	DP, 9	−3p, −22	X	
50	ccRCC	72/M	8	III (T_{3b},N_x,M_x)	2	DP, 30	−Y, +2, −3p, +5, +7, −13p, −13q	X	
51	ccRCC	74/F	8	III (T_{3b},N_x,M_x)	2	NED, 25	der(3)t(3;5), −14, −16q, +21	X	
52	ccRCC	80/M	10.5	III (T_{3b},N_x,M_x)	2	DP, 14	+X, −2, −3p, −3p, +3q, −5p, +7, −11q, +12q, +12q, −14q, −14, −15, +16, −21, −22	X	
53	ccRCC	55/M	12	III (T_{3b},N_0,M_0)	3	DP, 38	−3p, −4, −6, −8, −9, −10, −11, −13, −15, −17, −18, −19, −21	X	X
54	ccRCC	60/M	12	III (T_{3b},N_0,M_x)	2	NA	der(3)t(3;5)	X	
55	ccRCC	63/F	11	III (T_{3c},N_1,M_0)	2	AD, 48	−X, −1q, +2, −3, −4q, +5, +5(2), +5(3), +12, −14q, +16, −19	X	X
56	ccRCC	64/M	2.5	IV (T_{1a},N_0,M_1)	2	DOTD, 27	der(3)t(3;5)	X	
57	ccRCC	49/M	4	IV (T_{1a},N_0,M_1)	2	AD, 65	−Y, −3p, +7q	X	
58	ccRCC	37/M	15	IV (T_2,N_x,M_1)	2	DOTD, 10	−Y, −1p, +1q, der(3)t(3;5), −4, −9, −14, −18, −22	X	X
59	ccRCC	59/M	7	IV (T_{3b},N_x,M_1)	2	AD, 18	NA	X	
60	ccRCC	70/F	9	IV (T_{3b},N_0,M_1)	2	DOTD, 3	der(3)t(3;5), +7, −21	X	X
61	ccRCC	61/F	9	IV (T_{3b},N_0,M_1)	2	AD, 31	−3p, −8p	X	
62	ccRCC	57/M	9	IV (T_{3b},N_0,M_1)	2	DOTD, 28	−Y, −3p, +5q, −6q	X	
63	ccRCC	60/M	10	IV (T_{3b},N_0,M_1)	2	DOTD, 18	NA	X	
64	ccRCC	45/M	10	IV (T_{3b},N_0,M_1)	3	AD	+1q, −2q, −3, −4, +5q, −8p, −11q, −13, −14	X	
65	ccRCC	73/F	15	IV (T_{3b},N_x,M_1)	2	AD, 4	−X, −1p, −3p, −3p, −8, −14	X	
66	ccRCC	67/F	8	IV (T4,N_0,M_1)	2	DOTD, 11	−3p, −8p, +12	X	
67	ccRCC	59/F	9	IV (T4,N_x,M_1)	2	DOTD, 24	−1p, −3, −9, −14, −17p, +17q	X	
68	ccRCC	47/M	13	IV (T_2,N_1,M_1)	2	DOTD, 4	der(3)t(3;5), −4q, −8p, −9, −10q, −14	X	
69	ccRCC	36/M	10	IV (T_{3a},N_1,M_1)	3	DOTD, 2	−2q, −3, +3q, −4q	X	
70	ccRCC	55/F	4.5	IV (T_{3b},N_1,M_1)	2	AD	−1p, −3p, +7	X	
71	ccRCC	56/F	5	IV (T_{3b},N_1,M_1)	2	DOTD, 8	−3, +3q, −6q, +7	X	X
72	ccRCC	71/M	9	IV (T_{3b},N_1,M_1)	3	DOTD, 2	−Y, −3, +3q, −6q	X	X
73	ccRCC	53/F	8	IV (T_{3a},N_2,M_1)	3	DOTD, 12	−3p, +5, +7, −8p, +8q, −9p, +12, −17p, +17q, +20	X	
74	ccRCC	69/M	12	IV (T_{3b},N_2,M_1)	2	DOTD, 4	−3p, −4p, +5, −7, −8q, −10p, −17q	X	X
75	ccRCC	50/M	4.5	I (T_{1b},N_0,M_0)	1	NED, 25	−3		X
76	ccRCC	71/M	4.5	I (T_{1b},N_0,M_0)	1	NED, 8	−Y, −3, +5, +7q, −8q, −11q, +12, −14, +16, −18q, +20		X
77	ccRCC	61/M	4	III (T_{3b},N_x,M_x)	2	DOTD, 48	−3, +5, +20, +22		X
78	ccRCC	79/M	5	III (T_{3b},N_0,M_0)	2	NED, 39	−Y, +1q, +2, der(3)t(3;5), +5, −11q, +12, −14, +17q, +22		X
79	ccRCC	79/F	6	III (T_{3b},N_0,M_0)	2	NED, 25	−3p, −15q, −15		X
80	ccRCC	77/M	6	III (T_{3b},N_0,M_0)	2	DP, 27	−2, −3, +3q, −7q, −8p, +8q, −9, −14, −15, −17p, −18, −19q, +21		X
81	ccRCC	68/F	6	III (T_{3b},N_0,M_0)	1	DP, 50	−3p, −8p		X
82	ccRCC	74/M	7	III (T_{3a},N_x,M_x)	2	NED, 43	NA		X
83	ccRCC	64/M	7	III (T_{3a},N_x,M_x)	3	NA	NA		X
84	ccRCC	59/F	7.5	III (T_{3b},N_x,M_x)	2	NA	NA		X
85	ccRCC	67/M	7.5	III (T_{3b},N_1,M_x)	3	AD, 9	NA		X
86	ccRCC	63/F	6	IV (T_{3b},N_x,M_1)	2	AD, 17	der(3)t(3;5)		X
87	ccRCC	66/M	15	IV (T_{3b},N_2,M_x)	2	AD	NA		X

Abbreviations: M, male; F, female; NED, no evidence of disease; DOTD, died of tumor disease; AD, advanced disease; DP, disease progression.

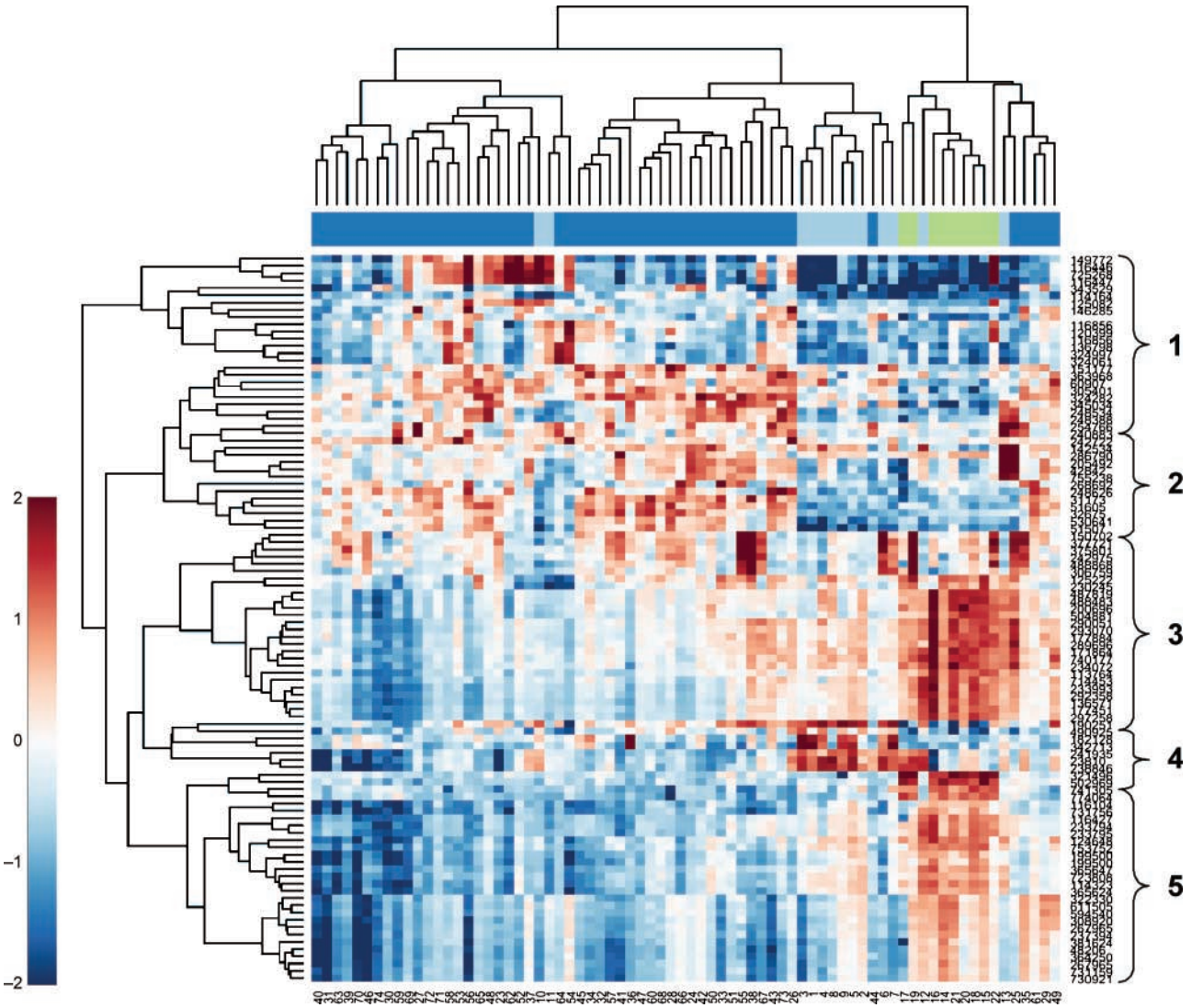

Fig. 1 Unsupervised hierarchical clustering of gene expression data from the 100 genes with highest variances. The different tumor types (*top; dark blue,* ccRCC; *light blue,* pRCC; *green,* chRCC) are distinguished by the pattern of up-regulation (*red*) and down-regulation (*blue*) of genes (listed vertically by their IMAGE IDs). *Numbers to the right,* gene groups given in the text.

highly up-regulated in most of the pRCC tissues. Among the latter were the genes for osteopontin (*SPP1*) and retinol binding protein 4 (*RBP4*). Cluster 5 genes were up-regulated in chRCC compared with ccRCC and pRCC. Among these were *HSF1*, *MYC* oncogene, and *CCND2*. Some genes were represented by several different clones on the arrays. For example, there were three different clones for *FN1* (IMAGE IDs 136798, 324997, and 324061) and two independent clones for *GAPD* (530641 and 51507). Different clones for each gene showed highly similar relative expression levels.

The dendrogram (Fig. 1) suggested that the ccRCC samples might be divided into two large subgroups encompassing samples (from *left* to *right*) 40 to 37 and 64 to 26, respectively. Gene expression differences between the subgroups were primarily found in gene clusters 1 (Fig. 1, *upper part*) and 3, including structural proteins like collagen (*COL3A1*) and fibronectin (*FN1*) and the gene for the nuclear receptor coactivator *NCOA4*, which has been shown to interact with the RET proto-oncogene in papillary thyroid carcinoma (30). A third small ccRCC subgroup was formed by samples 25, 29, 35, 49, and 61 (Fig. 1). Here, the tree topology suggested a relationship to the chRCC tumor types. This ccRCC subgroup was mainly characterized by differential gene expression in the genes from cluster 5. Histologic reanalysis of the tumor samples did not reveal common features that warranted distinction from the other ccRCC.

Classification Suggests Genes for Tumor Diagnosis. To investigate whether gene expression allows for a molecular classification of tumors, we used the prediction analysis for microarrays (27). Here, the performance of a classifier was assessed by the 10-fold cross-validated misclassification rate. A value of 5% to 10% was obtained for a wide range of choices for

the prediction analysis for microarray shrinkage variable. As shown in Fig. 2, the chRCC and ccRCC samples were classified with high confidence, whereas the classification of the pRCC seemed to be less certain. The lowest misclassification rate (2 of 74 samples misclassified) was obtained with an 80-gene classifier. Thirty-two of these genes were overlapping with those used for the hierarchical clustering (Table 2). Among them were *GAPD*, *VEGF*, *CXCL14*, *ADFP*, *SPP1*, and *CD4*. Several of these are key players in cancer and differentiation. *VEGF* is involved in angiogenesis; *CXCL14* is a cytokine that is frequently down-regulated in tumors (31); *ADFP* is a protein involved in cell differentiation and has been found to be highly overexpressed in ccRCC (32). The osteopontin gene (*SPP1*) is a target for *TP53* (33) and a lead marker for colon cancer progression (34). Other genes that were highly diagnostic for RCC type were the multiple drug resistance factor *MDR1*, several components of the respiratory chain (*COX7B*, *NDUFS4*, and *NDUFS6*), the gene for GTP-binding protein (*CDC42*), a component of the *RAS* oncogene signaling pathway, and the *KIT* oncogene.

A Primary Tumor Gene Expression Pattern Associated with Metastasis Formation. To fully analyze gene expression patterns within ccRCC, we tested for the association of the expression level of each gene with different clinicopathologic variables (Table 3). We detected gene expression patterns that were significantly associated with metastasis formation at the time of surgery (Supplementary Table S3) and patient survival (Supplementary Table S4). Among the most significantly deregulated genes in metastasized tumors were the human high-mobility group gene (*HMGA1*) and the mitochondrial dienoyl-CoA reductase (*DECR1*). These genes were also associated with patient survival. Consistent with other data (23), the gene for the GTP-binding protein (*RAGB*) was found up-regulated in metastasized tumors. Furthermore, genes belonging to gene families (*COL5A1*, *SLC13A3*, *SLC29A2*, *IGFBP3*, and *GUCY2C*) were associated with metastasis formation (this has been observed previously with other members of these families; refs. 20, 23). As in metastasized breast tumors (35), the gene for a peroxisomal enzyme catalyzing isomerization of fatty acids (*PECI*) was down-regulated in metastasized RCC. Twelve of the genes associated

Table 2 Genes and ESTs highly diagnostic for kidney tumor types

IMAGE ID	Gene
51605	*VEGF*
31173	*ANGPTL4*
32675	*CDC42*
324282	*ADFP*
305401	*HLA-DRB1*
345034	*CXCL14*
530641	*GAPD*
51507	*GAPD*
114164	*EST*
487819	*CEBPD*
321496	*PVALB*
502969	*IFI27*
241935	*SPP1*
23810	*SPP1*
238846	*TSPAN-1*
741305	*SLC9A1*
774064	*ATP6V0A4*
731756	*PRPH*
199500	*EST*
365647	*CD4*
114323	*EST*
365624	*NSPC1*
124648	*B3GNT6*
488483	*ZNF71*
200696	*EST*
113764	*EST*
233993	*EST*
136571	*EST*
177451	*RPL19*
297258	*RFWD1*
233794	*EST*
233795	*DMXL1*

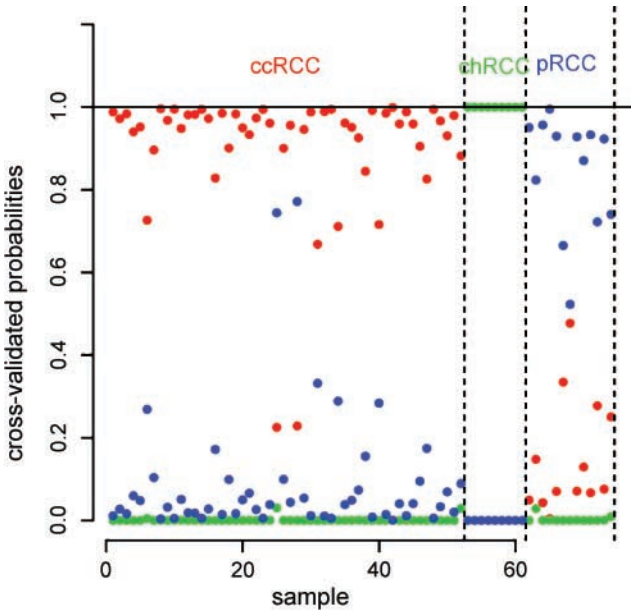

Fig. 2 Classification of RCC samples using prediction analysis for microarrays (27). Cross-validated classification probabilities (*Y axis*) are plotted for each tumor sample (*X axis; red,* ccRCC; *green,* chRCC; *blue,* pRCC).

Table 3 Numbers of differentially expressed genes in pairwise comparisons

Comparison	Class (*n*)	Class (*n*)	Genes	Experimental design	Estimated false discovery rate
Tumor-normal	ccRCC (25)	ccRCC (25)	1,181	Paired*	$q < 0.23$
Histologic type	NA	NA	1,224	Reference†	0.0067
ccRCC gain 5q	Yes (25)	No (25)	2	Reference‡	1
ccRCC grade	1 (5)	2 or 3 (47)	35	Reference‡	1
ccRCC metastasis	M_0 (17)	M1 (19)	85	Reference‡	0.1845
ccRCC progress	No (16)	Yes (30)	17	Reference‡	1
ccRCC stage	1 + 2 (15)	3 + 4 (37)	7	Reference‡	1
ccRCC net changes	NA	NA	57	Reference§	0.3343
ccRCC survival	NA	NA	45	Reference‖	0.4661

*Significance Analysis of Microarrays software package was used to identify differentially expressed genes.
†*F* test ($P < 0.005$).
‡*t* test ($P < 0.005$).
§Gene-wise linear model ($P < 0.005$).
‖Cox proportional hazard model ($P < 0.005$).

with tumor metastasis formation and patient survival corresponded to those used in the hierarchical clustering analysis (Fig. 1), indicating that the potential for metastasis formation is a prominent factor for the clustering of primary tumors.

Gene Expression Is Associated with Cytogenetic Abnormalities. To test for associations between gene expression and cytogenetic aberrations, we examined the correlation of the expression levels of any given gene with the copy number of the chromosomal arm where it is located. Of all genes on the microarrays, 2,968 mapped to chromosomal regions that were altered in at least 10% of the tumors. The expression of 136 of these was significantly associated with chromosomal copy number (linear model analysis, $P < 0.01$; estimated false discovery rate = 0.21). The highest numbers of gene expression change matched exactly the chromosome regions that are primarily affected in ccRCC (3p) and pRCC (7q, 16p, and 17q; Fig. 3*A*). For example, 15 of 83 genes in the 3p region were down-regulated in tumors with loss of 3p (Fig. 3*B*). Among these were *MAPKAPK3*, which is activated in all three MAPK cascades (36), and *PRKCD*, a protein kinase involved in B-cell signaling. Furthermore, significantly deregulated genes mapping to 7q were the *MET* proto-oncogene, which is associated with pRCC (37), and *MDR1* (an ABC transporter). A more detailed analysis revealed that *MDR1* is overexpressed only in pRCC, but not in ccRCC, with 7q amplification. Thus, the amplification of the chromosome arm 7q affects *MDR1* gene expression exclusively in one of two RCC types and may be involved in pRCC formation.

Deregulated Pathways in ccRCC. We hybridized labeled cDNA from 25 ccRCC with matched normal samples (Table 1) and used the Significance Analysis of Microarrays software (25) to identify deregulated genes. In total, 1,181 genes or ESTs (620 up-regulated and 561 down-regulated; estimated false discovery rate < 0.23) were differentially expressed (Supplementary Table S5). A comparison with our previous data (19) resulted in an 85% correspondence of up-regulation and down-regulation among the 702 genes that were present in both studies. Similarly, the deregulation pattern of 48 of 49 genes that overlapped with the data set of ref. 20 was consistent with the one identified in our ccRCC series. Evidence for the up-regulation of the integrin-mediated cell adhesion pathway was provided by several of its components (*ITGA3*, *ITGA5*, *ITGB1*, *ITGB8*, *CAV1*, and *CAVI2*), suggesting enhanced cellular communication in the tumor tissue. Furthermore, six of nine genes coding for glycolytic proteins (*PFK*, *TPI*, *GAPD*, *PGK*, *PGM*, and *ENO*) were up-regulated and two of those for gluconeogenesis (*ALDO* and *PCK*) were down-regulated. No gene regulation that conflicted with this tendency was observed. This finding is supported by measurements of enzyme activities in RCC (38). These and other gene expression changes (e.g., up-regulation of *VEGF* and *ADM*) could be a consequence of decreased oxygen supply within tumors. Thus, even with specific microarrays it is possible to gain a comprehensive insight into tumor-associated cellular processes and tumor biology. Notably, the *GAPD* gene, which is often used for normalization of quantitative real-time PCR measurements, was highly up-regulated in ccRCC (39), suggesting that its use as a housekeeping gene in RCC studies has to be considered with caution.

Validation. For validation of the microarray results, we examined the genes *LGALS3*, *VEGF*, *SPP1*, *APOE*, *BRF1*, and *CAV1* by quantitative real-time PCR analysis (Fig. 4). The data were normalized against *COPB* (similar results were obtained with *ACTB*). As expected from the microarray data, *VEGF*, *LGALS3*, and *CAV1* were up-regulated and *APOE* was down-regulated in ccRCC when compared with normal tissue. The former three genes are involved in tumor progression. However, the reason for the down-regulation of *APOE* in RCC is unknown. In mice, however, the abrogation of *APOE* was shown to result in increased cell proliferation and matrix formation (40), suggesting a link of *APOE* to tumor-related processes. The tumor type–specific gene expression of *SPP1* and *CAV1* corresponded with the microarray results. Notably, *SPP1* was up-regulated in pRCC but down-regulated in the other tumor types and is therefore a potent marker gene for pRCC. Similarly, *VEGF* and *APOE* expression levels remained invariant in pRCC, whereas they were consistently different in chRCC and ccRCC. *VEGF* expression was consistent with the microarray data, whereas *APOE* deregulation in chRCC was not evident from the array results. The expression of *LGALS3* differed largely between the tumor types, with a maximum 23-fold up-regulation in chRCC. As expected, *BRF1*, which was included for control reasons, was not

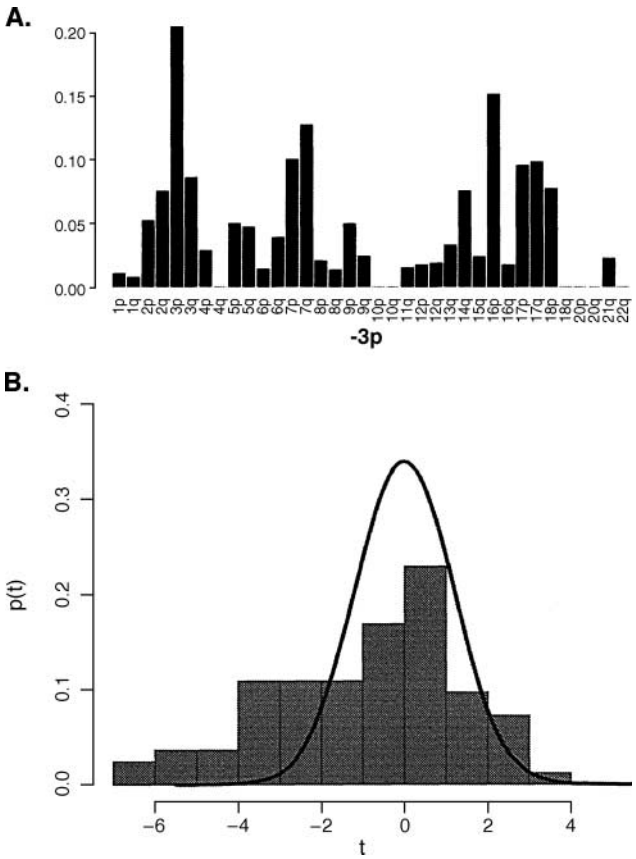

Fig. 3 *A,* correspondence of gene expression with chromosomal changes. *X axis,* chromosomal arm; *Y axis,* proportion of genes of which expression level is significantly ($P < 0.01$) associated with the copy number of a chromosome arm compared with the total number of genes on that chromosome arm and present on the renal carcinoma microarrays. *B,* association of gene expression and chromosomal aberration for chromosome 3p. The histogram shows the distribution of the two-sample *t* statistic (*Y axis*) for the genes located on chromosome 3p, comparing the tumors with and without loss of 3p. *Solid line,* null distribution estimated from permutations. A significant fraction of genes shows strongly negative values of *t* (*X axis*), indicating down-regulation in the tumors with loss of 3p.

differentially expressed between the tumor types or between tumor and normal tissues.

DISCUSSION

The present study comprises the largest number of tumor and normal samples that have been reported in microarray studies of RCC. Our data show the benefit of microarrays for tumor classification reflecting the differences in histogenesis, morphology, and biology between these RCC types at the molecular level. Furthermore, our gene expression data in ccRCC highlight the potential of microarray analysis for the identification of biologically relevant deregulated pathways.

We propose a set of 32 marker genes and ESTs that discriminated best among the three major types of RCC, providing candidates for a molecularly based differential diagnosis. Moreover, gene expression data identified molecular heterogeneity within a given tumor type. This is exemplified by genes with known oncogenic and cell adhesion functions that differentiate ccRCC into several subgroups. This finding is in agreement with other studies that report prognostically different subsets in renal cancer (20, 23) and might be the basis for a clinically meaningful subclassification.

Although our data revealed an association between primary tumor gene expression and metastatic potential in ccRCC, this was unexpected because our microarrays were designed mainly based on tumor-normal gene expression differences. Therefore, it is highly conceivable that we were only able to detect a fraction of genes linked with metastasis formation or prognostic variables. To account for this issue and to achieve maximum comparability with other data sets, we have started to use whole genome human cDNA microarrays containing 36,000 genes and ESTs to identify metastasis-related genes in RCC. However, this requires large, standardized, and well-fostered patient biopsy collections as well as a comprehensive and long-term patient assessment. These prerequisites, besides well-established microarray technology and quality control to achieve a maximum quality of the data, cannot be overestimated.

The common view of cancer progression through stepwise accumulation of genetic changes, followed by clonal selection, has recently been challenged (41, 42). It is intriguing to think of the capability of a tumor to metastasize as a property that is acquired early during tumor development. Our data support the idea that the propensity to metastasize is predefined by gene expression signatures in the primary tumors. We found a large number of genes that were significantly associated with metastatic potential and patient survival in RCC. Many of these genes were consistent with other data sets. Moreover, certain genes may play pivotal roles in metastasis formation in different tumor types (42). For example, down-regulation of the *PECI* gene in tumors is associated with metastasis formation in both RCC (this study) and breast cancer (35). Therefore, this gene may be a suitable target for approaches to prevent metastasis formation in various cancer types. We anticipate that further comprehensive microarray analyses using primary tumors will reveal more such promising candidate genes for future therapies.

The extent to which chromosomal aberrations in tumor cells influence gene expression levels has been a matter of considerable

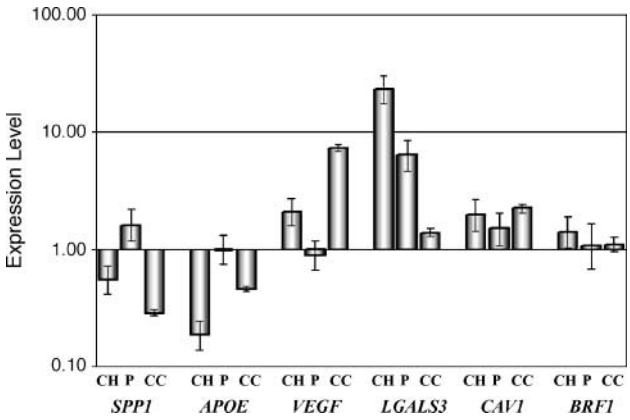

Fig. 4 Logarithmic expression levels (*Y axis*) of six genes in the three tumor types (*X axis; CH,* chRCC; *P,* pRCC; *CC,* ccRCC) determined by quantitative real-time PCR and normalized against *COPB*. *Bars*, SD.

debate (43, 44). Whereas there are classic examples for the association of oncogene expression levels with the amplification of certain chromosomal regions (45, 46), many of the genes associated with altered DNA copy numbers may be subject to dosage compensation effects. Nonetheless, we found that the expression levels of a substantial fraction of the genes are significantly correlated with chromosome copy number in RCC cells. For comparison, in a recent study of breast tumors (43), 12% of the variation in gene expression were directly attributable to variation in gene copy number. Thus, chromosomal aberrations affect gene expression levels to a certain extent. Many of the genes associated with chromosomal status are key players of cancer formation or progression, although others have not yet been associated with tumors and may be central to currently unknown tumorigenic processes. One particularly interesting example of the latter category is the expression pattern of the drug resistance gene *MDR1*, which was significantly up-regulated only in pRCC, but not in ccRCC, with 7q amplification. This indicates that several genes that are associated with chromosome status are mechanistically linked to the tumor formation process. Most of the genes, however, are either not expressed at all in the tumors or subject to mechanisms compensating for altered gene expression like transcriptional regulation, alternative splicing, epigenetic changes, or protein modification.

In conclusion, we detected gene expression patterns correlating with metastasis formation, patient survival, and cytogenetic data. Comparisons with other microarray data sets showed large correspondence of results obtained by different laboratories and array platforms. Thus, gene expression profiling provides a potent universal tool for a refined molecular diagnosis and prognostic evaluation. As more data are accumulating, gene or protein expression patterns will not only improve current diagnostic routines but also further reveal highly promising target genes for future tumor therapies.

ACKNOWLEDGMENTS

We thank Jan Mollenhauer and Patricia McCabe for the critical reading of the article and the Resource Center/Primary Databases for providing clones.

REFERENCES

1. Fleming S. Genetics of kidney tumours. Forum (Genova) 1998; 8:176–84.

2. Thoenes W, Störkel S, Rumpelt HJ, Moll R. Cytomorphological typing of renal cell carcinoma—a new approach. Eur Urol 1990;18 Suppl 2:6–9.

3. Storkel S, Eble JN, Adlakha K, et al. Classification of renal cell carcinoma. Workgroup No. 1. Union Internationale Contre le Cancer (UICC) and the American Joint Committee on Cancer (AJCC). Cancer 1997;80:987–9.

4. Kovacs G. Molecular differential pathology of renal cell tumours. Histopathology 1993;22:1–8.

5. Phillips JL, Pavlovich CP, Walther M, Ried T, Linehan WM. The genetic basis of renal epithelial tumors: advances in research and its impact on prognosis and therapy. Curr Opin Urol 2001;11:463–9.

6. Kovacs G, Frisch S. Clonal chromosome abnormalities in tumor cells from patients with sporadic renal cell carcinomas. Cancer Res 1989; 49:651–9.

7. Gunawan B, Huber W, Holtrup M, et al. Prognostic impacts of cytogenetic findings in clear cell renal cell carcinoma: gain of 5q31-qter predicts a distinct clinical phenotype with favorable prognosis. Cancer Res 2001;61:7731–8.

8. Kovacs G, Füzesi L, Emanual A, Kung HF. Cytogenetics of papillary renal cell tumors. Genes Chromosomes Cancer 1991;3:49–255.

9. Gunawan B, von Heydebreck A, Fritsch T, et al. Cytogenetic and morphologic typing of 58 papillary renal cell carcinomas: evidence for a cytogenetic evolution of type 2 from type 1 tumors. Cancer Res 2003;63:6200–5.

10. Gunawan B, Bergmann F, Braun S, et al. Polyploidization and losses of chromosomes 1, 2, 6, 10, 13, and 17 in three cases of chromophobe renal cell carcinomas. Cancer Genet Cytogenet 1999;110:57–61.

11. Brieger J, Weidt EJ, Schirmacher P, Storkel S, Huber C, Decker HJ. Inverse regulation of vascular endothelial growth factor and VHL tumor suppressor gene in sporadic renal cell carcinomas is correlated with vascular growth. An *in vivo* study on 29 tumors. J Mol Med 1999; 77:505–10.

12. Takahashi A, Sasaki H, Kim SJ, et al. Identification of receptor genes in renal cell carcinoma associated with angiogenesis by differential hybridization technique. Biochem Biophys Res Commun 1999;257:855–9.

13. Ishikawa J, Maeda S, Umezu K, Sugiyama T, Kamidono S. Amplification and overexpression of the epidermal growth factor receptor gene in human renal-cell carcinoma. Int J Cancer 1990;45: 1018–21.

14. Moch H, Sauter G, Gasser TC, et al. EGF-r gene copy number changes in renal cell carcinoma detected by fluorescence *in situ* hybridization. J Pathol 1998;184:424–9.

15. Lager DJ, Slagel DD, Palechek PL. The expression of epidermal growth factor receptor and transforming growth factor α in renal cell carcinoma. Mod Pathol 1994;7:544–8.

16. Drabkin HA, Bradley C, Hart I, Bleskan J, Li FP, Patterson D. Translocation of c-*myc* in the hereditary renal cell carcinoma associated with a t(3;8)(p14.2;q24.13) chromosomal translocation. Proc Natl Acad Sci U S A 1985;82:6980–4.

17. Yao M, Shuin T, Misaki H, Kubota Y. Enhanced expression of c-*myc* and epidermal growth factor receptor (C-erbB-1) genes in primary human renal cancer. Cancer Res 1988;48:6753–7.

18. Moch H, Schraml P, Bubendorf L, et al. High-throughput tissue microarray analysis to evaluate genes uncovered by cDNA microarray screening in renal cell carcinoma. Am J Pathol 1999;154:981–6.

19. Boer JM, Huber WK, Sültmann H, et al. Identification and classification of differentially expressed genes in renal cell carcinoma by expression profiling on a global human 31,500-element cDNA array. Genome Res 2001;11:1861–70.

20. Takahashi M, Rhodes DR, Furge KA, et al. Gene expression profiling of clear cell renal cell carcinoma: gene identification and prognostic classification. Proc Natl Acad Sci U S A 2001;98:9754–9.

21. Gieseg MA, Cody T, Man MZ, Madore SJ, Rubin MA, Kaldjian EP. Expression profiling of human renal carcinomas with functional taxonomic analysis. BMC Bioinformatics 2002;3:26.

22. Higgins JP, Shinghal R, Gill H, et al. Gene expression patterns in renal cell carcinoma assessed by complementary DNA microarray. Am J Pathol 2003;162:925–32.

23. Vasselli JR, Shih JH, Iyengar SR, et al. Predicting survival in patients with metastatic kidney cancer by gene-expression profiling in the primary tumor. Proc Natl Acad Sci U S A 2003;100:6958–63.

24. Huber W, von Heydebreck A, Sultmann H, Poustka A, Vingron M. Variance stabilization applied to microarray data calibration and to the quantification of differential expression. Bioinformatics 2002;18 Suppl 1:S96–104.

25. Tusher VG, Tibshirani R, Chu G. Significance analysis of microarrays applied to the ionizing radiation response. Proc Natl Acad Sci U S A 2001;98:5116–21.

26. Ihaka R, Gentleman R. A language for data analysis and graphics. J Comput Graph Stat 1996;5:299–314.

27. Tibshirani R, Hastie T, Narasimhan B, Chu G. Diagnosis of multiple cancer types by shrunken centroids of gene expression. Proc Natl Acad Sci U S A 2002;99:6567–72.

28. Storey JD, Tibshirani R. SAM thresholding and false discovery rates for detecting differential gene expression in DNA microarrays.

In: Parmigiani G, Garrett ES, Irizarray RA, Zeger SL, editors. The analysis of gene expression data. Methods and software. New York: Springer; 2003.

29. Pfaffl MW. A new mathematical model for relative quantification in real-time RT-PCR. Nucleic Acids Res 2001;29:e45.

30. Bongarzone I, Butti MG, Coronelli S, et al. Frequent activation of ret proto-oncogene by fusion with a new activating gene in papillary thyroid carcinomas. Cancer Res 1994;54:2979–85.

31. Hromas R, Broxmeyer HE, Kim C, et al. Cloning of BRAK, a novel divergent CXC chemokine preferentially expressed in normal versus malignant cells. Biochem Biophys Res Commun 1999;255:703–6.

32. Weinschenk T, Gouttefangeas C, Schirle M, et al. Integrated functional genomics approach for the design of patient-individual antitumor vaccines. Cancer Res 2002;62:5818–27.

33. Morimoto I, Sasaki Y, Ishida S, Imai K, Tokino T. Identification of the osteopontin gene as a direct target of TP53. Genes Chromosomes Cancer 2002;33:270–8.

34. Agrawal D, Chen T, Irby R, et al. Osteopontin identified as lead marker of colon cancer progression, using pooled sample expression profiling. J Natl Cancer Inst 2002;94:513–21.

35. van't Veer LJ, Dai H, van de Vijver MJ, et al. Gene expression profiling predicts clinical outcome of breast cancer. Nature 2002;415: 530–6.

36. Ludwig S, Engel K, Hoffmeyer A, et al. 3pK, a novel mitogen-activated protein (MAP) kinase-activated protein kinase, is targeted by three MAP kinase pathways. Mol Cell Biol 1996;16:6687–97.

37. Schmidt L, Duh FM, Chen F, et al. Germline and somatic mutations in the tyrosine kinase domain of the MET proto-oncogene in papillary renal carcinomas. Nat Genet 1997;16:68–73.

38. Steinberg P, Storkel S, Oesch F, Thoenes W. Carbohydrate metabolism in human renal clear cell carcinomas. Lab Invest 1992; 67:506–11.

39. Vila MR, Nicolas A, Morote J, de I, Meseguer A. Increased glyceraldehyde-3-phosphate dehydrogenase expression in renal cell carcinoma identified by RNA-based, arbitrarily primed polymerase chain reaction. Cancer 2000;89:152–64.

40. Chen G, Paka L, Kako Y, Singhal P, Duan W, Pillarisetti S. A protective role for kidney apolipoprotein E. Regulation of mesangial cell proliferation and matrix expansion. J Biol Chem 2001;276:49142–7.

41. Bernards R, Weinberg RA. A progression puzzle. Nature 2002; 418:823.

42. Ramaswamy S, Ross KN, Lander ES, Golub TR. A molecular signature of metastasis in primary solid tumors. Nat Genet 2003;33: 49–54.

43. Pollack JR, Sorlie T, Perou CM, et al. Microarray analysis reveals a major direct role of DNA copy number alteration in the transcriptional program of human breast tumors. Proc Natl Acad Sci U S A 2002;99: 12963–8.

44. Albertson DG, Collins C, McCormick F, Gray JW. Chromosome aberrations in solid tumors. Nat Genet 2003;34:369–76.

45. Alitalo K, Schwab M, Lin CC, Varmus HE, Bishop JM. Homogeneously staining chromosomal regions contain amplified copies of an abundantly expressed cellular oncogene (c-*myc*) in malignant neuroendocrine cells from a human colon carcinoma. Proc Natl Acad Sci U S A 1983;80:1707–11.

46. Hinds PW, Dowdy SF, Eaton EN, Arnold A, Weinberg RA. Function of a human cyclin gene as an oncogene. Proc Natl Acad Sci U S A 1994; 91:709–13.